GENE TARGETING IN HEMOSTASIS. ALPHA$_2$-ANTIPLASMIN

H.R. Lijnen

Center for Molecular and Vascular Biology, University of Leuven, Campus, Gasthuisberg, O & N, Herestraat 49, B-3000 Leuven, Belgium

TABLE OF CONTENTS

1. ABSTRACT

Apha$_2$-antiplasmin (AP), the main physiological plasmin inhibitor in mammalian plasma, is a 70 kDa single chain serpin (<u>ser</u>ine <u>p</u>roteinase <u>in</u>hibitor) with reactive site peptide bond Arg-Met. It inhibits plasmin very rapidly (second-order inhibition rate constant of $= 2 \times 10^7$ M^{-1}.s^{-1}) following formation of an inactive 1:1 stoichiometric complex. The high reaction rate requires the presence of a free active site and free lysine-binding site(s) in plasmin. The pathophysiologic relevance of AP is suggested by the finding that homozygous deficient patients show a bleeding tendency; heterozygotes, in contrast, frequently have no or only mild bleeding complications. Inactivation of the AP gene in mice was achieved by replacing, via homologous recombination in embryonic stem cells, a 7 kb genomic sequence encoding the entire murine protein with the *neomycin resistance* expression cassette. Homozygous AP deficient mice display normal fertility, viability and development. They have an enhanced endogenous fibrinolytic capacity without overt bleeding; this is reflected by a higher spontaneous lysis rate of experimental pulmonary emboli, by a reduced fibrin deposition in the kidneys following challenge with endotoxin, by more limited photochemically induced arterial thrombosis, and by reduced infarct size following induction of focal cerebral ischemia by ligation of the left middle cerebral artery. In a vascular injury restenosis model, AP deficiency has no significant effect on smooth muscle cell migration and neointima formation. These data suggest that, at least in the murine system, the main role of alpha$_2$-antiplasmin is in regulating plasmin activity in the circulating blood and in controlling intravascular fibrinolysis.

2. INTRODUCTION

The fibrinolytic (plasminogen/plasmin) system contains a proenzyme, plasminogen, that is converted to the active enzyme, plasmin, by tissue-type (t-PA) or urokinase-type (u-PA) plasminogen activator. Inhibition of the fibrinolytic system may occur at the level of plasmin or at the level of plasminogen activators. For a long time, it was accepted that there were essentially two functionally important plasmin inhibitors in plasma: an immediately reacting inhibitor and a slower reacting inhibitor identical to alpha$_2$-macroglobulin and alpha$_1$-antitrypsin, respectively. About 25 years ago, another plasmin inhibitor, alpha$_2$-antiplasmin (AP) or alpha$_2$-plasmin inhibitor was identified in human plasma. On activation of plasminogen in plasma, plasmin is preferentially bound by this inhibitor. The complete activation of plasminogen (concentration about 2 µM), resulting in saturation of
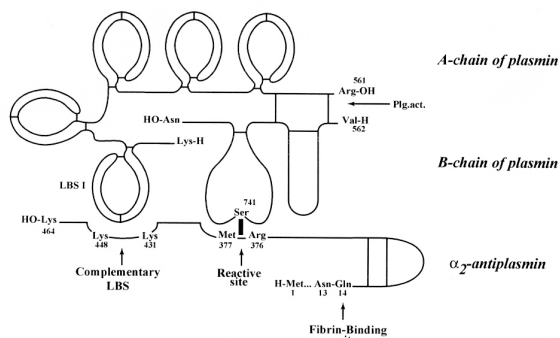
Figure 1. Schematic representation of the plasmin-alpha₂ antiplasmin complex. LBSI, indicates the high affinity lysine-binding site; Plg.act., indicates the site of cleavage in plasminogen for plasminogen activators.

alpha₂-antiplasmin (concentration about 1 µM), must occur before the excess plasmin is neutralized by other inhibitors (1). AP, like many other plasma proteinase inhibitors, has a broad in vitro inhibitory spectrum, but its physiologic role as an inhibitor of proteinases other than plasmin seems negligible.
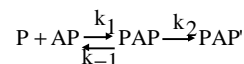
3. BIOCHEMISTRY

3.1. Physicochemical characterization

Human alpha₂-antiplasmin (AP) is a single-chain protein of 70 kDa containing about 13% carbohydrate (attached at Asn^{99}, Asn^{268}, Asn^{282} and Asn^{289}). The molecule consists of 464 amino acids and contains two disulfide bridges (2,3) ("figure 1"). Subsequently, it was however suggested that AP contains only one Cys^{43}-Cys^{116} disulfide bond and possibly two unpaired cysteines (Cys^{76} and Cys^{125}) (4). AP belongs to the <u>se</u>rine proteinase <u>in</u>hibitor family (serpins). Two molecular forms are present in about equal amounts in purified preparations of the inhibitor: a native 464 residues long inhibitor with amino-terminal methionine (Met^1-AP) and a 12 amino acids shorter form with amino-terminal asparagine (Asn^{13}-AP) (5). It is not known whether Asn^{13}-AP is present in the circulating blood or whether it is generated in vitro. The amino-terminal Gln^{14}-residue of AP can cross-link to A-alpha chains of fibrin, in a process which requires Ca^{2+} and is catalyzed by activated coagulation factor XIII (6) (figure 1). Asn^{13}-AP is more efficiently cross-linked to fibrin than Met^1-AP (7).

The concentration of the inhibitor in normal plasma is about 7 mg/dL (about 1 µM) (8). The in vivo half-life of AP is 2.6 days, whereas the plasmin-AP complex disappears from plasma with a half-life of about half a day (9). The inhibitor in normal plasma is heterogeneous and consists of functionally active and inactive material. Complete activation of the plasminogen present in normal plasma converts only about 70% of the antigen into a complex with plasmin; 30% of the inhibitor-related antigen appears to be functionally inactive or slower reacting. These two forms of the inhibitor differ in binding to plasminogen. The form that does not bind remains an active plasmin inhibitor (10) but reacts much slower with plasmin; this form lacks a 26-residue peptide from the

carboxy-terminal end (11). This peptide inhibits the interaction of AP with plasmin, which suggests that it contains the plasminogen-binding site. From the ratio of these forms in the plasma of pregnant women subjected to extensive plasmapheresis, it was concluded that the plasminogen-binding form of AP is primarily synthesized and becomes partly converted to the non-plasminogen-binding form in the circulating blood (12).

3.2. Mechanism of interaction with plasmin

In purified systems and in plasma, AP forms a 1:1 stoichiometric complex with plasmin that is devoid of proteinase or esterase activity. Kinetic studies revealed that the disappearance of plasmin activity after addition of excess AP does not follow first-order kinetics (13-15). Even though most of the plasmin is rapidly inactivated, the process slowly proceeds toward completion. This time course of the reaction is compatible with a kinetic model composed of two successive reactions: a fast, reversible second-order reaction followed by a slower, irreversible first-order transition. The model can be represented by the following:

$$P + AP \underset{k_{-1}}{\overset{k_1}{\rightleftharpoons}} PAP \overset{k_2}{\rightarrow} PAP'$$

where P is plasmin, AP is alpha₂-antiplasmin, PAP is a reversible inactive complex and PAP' is an irreversible inactive complex.

The second-order rate constant (k_1) is 2 to 4 x 10^7 $M^{-1}.s^{-1}$. This is among the fastest protein-protein reactions described. The dissociation constant of the reversible complex is 2 x 10^{-10} M. The half-time of the first-order transition, PAP → PAP', is 166 seconds, corresponding to a k_2 value of 4.2 x $10^{-3}s^{-1}$. Christensen and Clemmensen (13) reported a value of 6.5 x 10^{-3} s^{-1} for k_2.

Plasmin molecules with a synthetic substrate bound to their active site or with 6-aminohexanoic acid bound to their lysine-binding sites do not react or only react slowly with AP (10,14). The first step of the process thus clearly depends on the presence of a free lysine-binding site and active site in the plasmin molecule. This was further substantiated by studying the kinetics of the reaction between AP and a low molecular weight form of plasmin lacking the lysine-binding sites in the A-chain (15). The reaction scheme is identical to that observed with normal plasmin, but the rate constant of the first step is about 60 times lower and is only slightly inhibited by 6-aminohexanoic acid. These findings show that the first reversible step in the reaction between plasmin and AP can be divided into two parts: a reaction between the lysine-binding sites in the plasmin A chain and the plasmin(ogen)-binding site in AP, and subsequently a reaction between the active site in the B-chain of plasmin and the reactive site in AP. Because the reaction rate is strongly dependent on the availability of free lysine-binding sites, the main pathway is probably a consecutive reaction in this order. From competition experiments with plasminogen fragments containing lysine-binding sites, it appeared that the high-affinity lysine-binding sites situated in kringles 1 to 3 of the plasmin A chain are mainly responsible for the interaction with AP (16).

Plasmin and AP thus form a stoichiometric 1:1 complex of about 140 kDa. A nondisulfide-bonded peptide (8 kDa) is released concomitantly with complex formation. Upon disulfide bond reduction, the complex is dissociated in two parts : an intact plasmin A chain (60 kDa), and a stable complex between the plasmin B chain and AP (80 kDa), provided the complex formation is performed in excess AP (17). The reactive site peptide bond in AP cleaved by plasmin consists of Arg^{376}-Met^{377}. A covalent bond is formed between the active site seryl residue in plasmin and the reactive site arginyl residue in the inhibitor (figure 1). Site-directed mutagenesis studies revealed that deletion of the P_1' residu Met^{377} does not affect the ability of AP to inhibit plasmin or trypsin, whereas deletion of the P_1 residue Arg^{376} results in loss of the inhibitory capacity against plasmin, trypsin and thrombin but generates an effective elastase inhibitor (18).

In the murine system, plasmin inhibition by AP is equally rapid as in the human system, and the inhibitor in plasma also occurs in a plasminogen-binding and a non-plasminogen-binding form (19).

In plasma, the reaction rate between plasmin and AP may be reduced by the presence of proteins such as histidine-rich glycoprotein or fibrinogen,which interact with the lysine-binding sites of plasmin(ogen). The half-life of plasmin molecules on the fibrin surface, which are protected from inhibition because the lysine-binding sites and active site are occupied, is estimated to be two to three orders of magnitude longer than that of free plasmin (20).

3.3. Gene structure

The gene for human AP, located on chromosome 17 p 13 (21), is approximately 16 kb and contains 10 exons (22). The amino-terminal region of the protein, comprising the fibrin cross-linking site is encoded by exon IV, whereas both the reactive site and the plasminogen-binding site in the carboxy-terminal region are encoded by exon X.

4. PATHOPHYSIOLOGY

4.1. Congenital alpha₂-antiplasmin deficiency

The first case of congenital homozygous AP deficiency was described in a patient who presented with a hemorrhagic diathesis (23). Several cases of heterozygosity have been described with no or only mild bleeding symptoms (24). The AP levels in all heterozygotes described thus far are consistently between 40 and 60 percent of normal. Antigen and activity levels usually correspond well, suggesting that the deficiency is due to decreased synthesis of a normal AP molecule. The bleeding tendency in these patients may be due to premature lysis of hemostatic plugs, because in the absence of AP, the half-life of plasmin molecules generated on the fibrin surface is considerably prolonged.

The molecular defect in AP Okinawa was identified as a trinucleotide deletion in exon VII leading to deletion of Glu^{137} in the protein (25). In AP Nara insertion of a cytidine nucleotide in exon X leads to a shift in the reading frame of the mRNA resulting in deletion of the carboxy-terminal 12 amino acids of native AP and replacement with 178 unrelated amino acids (26). These mutations may lead to the deficiency by affecting the folding of the protein into the native configuration and thereby blocking its intracellular transport from the endoplasmatic reticulum to the Golgi complex (25).

Generation of AP-deficient mice (cf. below) revealed that they develop and reproduce normally; they have an enhanced endogenous fibrinolytic capacity without overt bleeding. The absence of a bleeding phenotype in these mice, in contrast to man, may reflect the fact that the coagulation system adequately prevents bleeding if the fibrinolytic system is not dramatically challenged (27).

4.2. Acquired alpha₂-antiplasmin deficiency

The serum level of AP is significantly decreased in liver cirrhosis and in several other liver diseases. Teger-Nilsson and coworkers (28) reported a mean value of 73 ±15% for liver cirrhosis (controls, 100 ± 8%), and Aoki and Yamanaka found values of 4.24 ± 0.87 mg/dL and 2.56 ± 0.87 mg/dL for compensated and decompensated liver cirrhosis, respectively (controls, 6.2 ± 0.8 mg/dL) (29). Thus, the decreased level of AP may be an important factor in the increased fibrinolytic activity observed in liver cirrhosis. Moreover, it is likely that the liver is the organ of synthesis or storage of AP (30).

Decreased levels of AP have also been reported in patients with disseminated intravascular coagulation and some forms of renal disease (31). AP levels may be significantly reduced in patients undergoing thrombolytic therapy as a result of systemic activation of the fibrinolytic system. Following intravenous infusion of either recombinant t-PA or streptokinase in patients with acute myocardial infarction, the decrease of AP is significantly greater in the streptokinase group (32).

4.3. Dysfunctional alpha₂-antiplasmin

An abnormal AP associated with a serious bleeding tendency was found in two siblings in a Dutch family (AP Enschede). These individuals have 3% of normal functional activity and 100% of normal antigen levels (33). Their apparently heterozygous parents have 50% functional activity and 100% antigen levels. The ability of the abnormal AP to reversibly bind plasmin or plasminogen is not affected, but it is converted from an inhibitor of plasmin to a substrate. The molecular defect of AP Enschede, revealed by sequencing of cloned genomic DNA fragments, consists of the insertion of an extra alanine residue (GCG insertion) 7 to 10 positions on the amino-terminal side of the P_1 residue (Arg 376) (34). This 3-bp in-frame insertion within the gene was identified in 2 heterozygotes and in their 2 homozygous children.

5. GENE TARGETING

5.1. Characterization of the murine alpha₂-antiplasmin gene

By alignment of murine genomic nucleotide sequences and comparison with the mouse *alpha₂-antiplasmin* cDNA (35) the 3'-end of exon 1 and exons 2 through 10 were located (figure 2). Comparison of the mouse and human *AP* gene revealed that exons 2 through 9
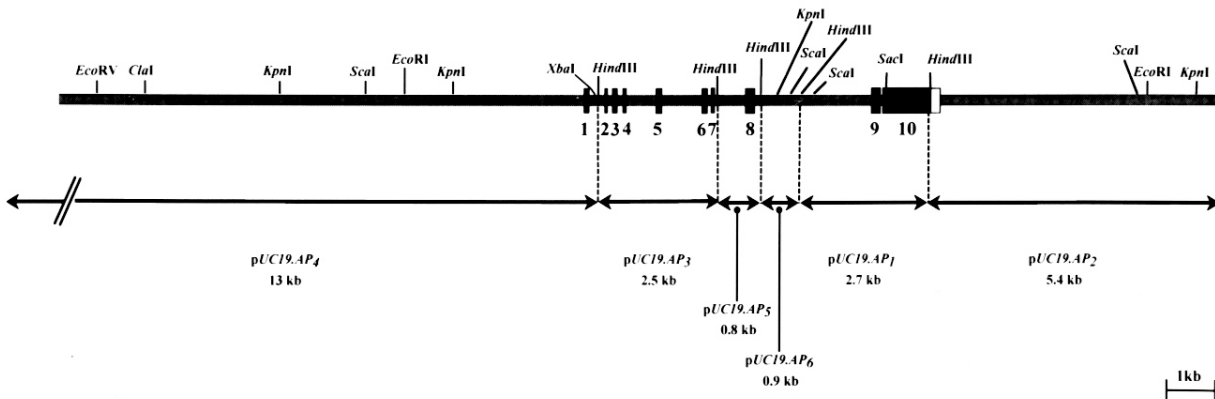
Figure 2. Schematic representation of the murine *AP* gene showing the location of each of the available genomic fragments subcloned in pUC19. Shaded areas in the gene represent intron sequences; black boxes represent coding exon sequences; open boxes represent non-coding exon sequences (reproduced from ref. 36, with permission).

have identical size and intron-exon boundaries obeying the GT/AG rule. The 5' boundary of exon 10 is identical in both genes while its 3' non-coding region is extended by 64 bp in the human gene. Introns 2, 3, 6 and 8 have similar sizes; intron 1 is 6-fold smaller and introns 5, 7 and 9 are 2- to 3-fold smaller in the mouse, while intron 4 is about 2-fold larger (36).

The longest open reading frame of the mouse *AP* gene, initiating in exon 2, encodes a 491 amino acid protein. The amino-terminal amino acid sequence of murine AP purified from plasma is

Val-Asp-Leu-Pro-Gly—

The amino-terminal Val, which corresponds to residue 28 of the protein, is encoded within exon 3, as is the amino-terminal Met of mature human AP.

Nucleotide sequence alignment of the human *AP* promoter, and the 5' part of the structural gene (GenBank M20781 and M20782) with sequences determined from p*UC19* subclones identified exon 2, intron 1 and the 3' end of exon 1 in the murine gene. Neither the 5' boundary of exon 1 nor the mouse equivalent of the human TATA box could be identified in this way. The nucleotide sequence at the 5' end of exon 1 (figure 2) revealed 2 differences (positions 1046 and 1050) with the published sequence (35).

Analysis of the mouse upstream genomic region identified an 18-bp direct repeat (with 4 mismatches), flanking a sequence located approximately 370 bp from the first exon (DR on figure 3) that comprises a region of simple repetitive DNA with the motif (TGG)n. Variable lengths of the (TGG)n repeat (30 to 140 bp) were observed by sequencing subcloned DNA or PCR amplification products generated on genomic DNA from RW4 or R1 ES cells. This might have resulted from rearrangements during cloning or from errors made within the (TGG)n sequence by the PCR or sequencing enzymes. Evidence against other putative rearrangements of the genomic sequences during

cloning procedures was provided by amplification of identical fragments in PCR reactions involving different primer combinations hybridizing upstream or downstream of or spanning the (TGG)n region, performed in parallel on pUC19.AP4 and on mouse genomic DNA. PCR with primers spanning the (TGG)n region was performed using a hot start PCR procedure. A truncated member of the B2 dispersed repeat family with intact A box, (Genbank K00132) was found on the antisense strand (position 5-49 in figure 2). No putative TATAA box was identified except for a putative TACA box (figure 2), located at coordinate 173 bp; such a sequence is shown in other genes to drive transcription initiation (37).

It is not clear at the present time where the transcription initiation site is located. Several attempts at locating it by primer extension have failed. However, RT-PCR analyses were performed on liver and kidney mRNAs with various primer combinations derived from the sequence between coordinates 1 and 1069 bp (figure 2) or from the published cDNA: amplified fragments were observed for all combinations into which the 5' primer extended up to bp 665, that is 370 bp upstream from the published cDNA 5' end.

5.2. Targeting of the murine *alpha$_2$-antiplasmin* gene

A homologous sequence of in total 8.3 kb was introduced in the parental p*PNT* vector which contains a *neomycin phosphotransferase* and a *Herpes simplex virus thymidine kinase* expression cassette, yielding the targeting vector p*PNT.alpha$_2$-AP* as outlined below and illustrated in figure 4. In a first step, a 4.5 kb *Eco*RI fragment containing a part of exon 10 and 3' flanking region was prepared from the plasmid p*UC19.AP$_2$*. The exon 10 fragment represents 3'-untranslated sequence starting at the *Hind*III site located 380 bp downstream from the STOP codon. This fragment was then ligated into EcoRI-restricted p*UC19* yielding p*UC19.AP$_2$*E(7.3 kb). The 4.5 kb *Kpn*I-*Eco*RI fragment from p*UC19.AP$_2$E* was then ligated into p*PNT* digested with KpnI and EcoRI, yielding p*PNT.AP$_2$* (12.8 kb).

Subsequently, a 3.7 kb *Hind*III-EcoRI fragment containing part of intron 1, exon 1 and approximately 2.8 kb of 5' flanking region was prepared from p*UC19.AP$_4$*.

Alpha₂-antiplasmin

A box

```
  1   GGATCCTTTG CAAGAGCAGC CAGTGTTCTT ACCCACTGAG CCCATCTCTA AGCCCCACAC CCAGCTTCTT  B2
 71   TGATACAAGG TCTGGTAGCT CAAACTTGAT ATGCAGCCGA GGAGGTTGAC CTGGTATTCC CTACCTACCC
141   TCTTCTCTCT ACCTTCCAAG TGCTGATATT ATACATAGGC ATGGATAGTC ATGCCCACCA GTTTGCCTTG
211   ATGGCACCAG AGTCAGGAAA GTCCAAACCT GGTAGTTGCA AACACAGCAA GAGGGTAGAG GCAGCCATTG
281   TCCTCTGGCT GCCTTGGATA CAGAGCTTCT GGGTTGGGTG GCCTTGGGTC AGTTTTCCGA ATGGTTCACC
351   CTTGGGGAAA GGGAACACTG CTGAAGAGGT GGGACCCTGG GAGGGCCGGG CCTCCAGCTG GGTCTCTCCA  DR
421   GCCCTCGCCT TGGAACCTAG GCTGGAGGGA GCCAACCAGG ATCCTGGACT GCTACAGTTA GGTGAACAGG
491   CTCTGCAGCC TCCCCTTCCC TTGGTAGCTG TGGTGGTGGT GGTGGTGGTG GTGGTGGTGG TGGTGGTGGT
561   GGTGGTGGTG GTAGTGGTGG TGGTGGTGGT GGTGGTGGTG GTGGTGGTGG TGGTGGTGGT AGTGGTGGTG
631   GTGGTGGTGG TGGTGGTGGT GGTGGTGGTG GACTTTGGCT GTGACTCTGG AGCCCGACTC TGCTGCCTTA  DR
701   CACAGGCCAC ACAGCCTCTC TGAGCCTCAC TGACTGTGGA TAATCCCCTA TGTTGAGGGA TCATTAGAAG
771   GCTTGCGCAG GCCCAACCTC CTCACTTATC TGCGTCCTGT AAACCCCTTC TCCAGGCTCA GGCAGGGTTC
841   TGGGTAGCCT TGATGGAAAA GGGTCTTCTG GCCCCCATAT CAATGTTTAA CCGGATGTAC AGGTCAATAT
911   TTACCAGCAC TGAACACAAG CTGAACGGGG GTTGGCTGAG AGCAAAGGTC CTGTGGGAGG AGAGAGCTAG
981   GCCCTGCTGG CTGCACTGGG GAGCGTGGGG AGCAAGCTGG TCCAGGAGAA CACCGTGTGC TGCGTgTCTg  Exon 1
1051  CGCTAAGAAG CCTGAAGAGG TAGGATGGAG ....... intron 1 (971 bp) ...... GAACTAACAC
2031  TCCCTGTTAG GAACATGGCA CTGCTCCGGG GGCTCCTCGT ACTCAGCTTG TCCTGCCTGC AAGGTCCCTG  Exon 2
2101  TTTCACG
```

Figure 3. Nucleotide sequence of the 5' end of the murine *AP* gene comprising approximately 1 kb of 5' flanking sequence, exon 1, intron 1 (shown in part) and exon 2. The ATG codon in exon 2 is underlined. The (TGG)n repeat sequence, shown at its maximum observed length, is indicated with a dotted line. An 18-bp direct repeat (DR) is indicated by arrows below the sequence, and a B2 repeated element (B2), located on the antisense strand, is underlined. A conserved A box found in RNA polymerase III promoters and a putative TACA box are indicated. Comparison with the published murine AP cDNA sequence (GenBank AC Z36774) revealed a nucleotide insertion (G) at position 1046 (lower case + underlined) and a C -> G substitution at position 1050 (lower case) in exon 1. The first 6 nucleotides of the published GenBank cDNA sequence (*Eco*RI site) were not considered in the comparison. The 5' end of exon 1, which was not identified, was left open (reproduced from ref. 36, with permission). The nucleotide sequence as shown in this figure has been submitted to the GenBank data bank with accession number Y12312.

This fragment was ligated into HindIII-EcoRI-restricted pBluescript II KS (p*BKS*), yielding p*BKS.AP₄HE* (6.6 kb). Then, p*BKS.AP₄HE* was digested with XhoI and NotI and a 3.7 kb fragment was ligated into NotI-XhoI digested p*PNT.AP₂*, yielding p*PNT.alpha₂-AP*. Correct orientation of the 5' and 3' flanking region was verified by appropriate restriction digest analysis and PCR. In the targeting vector p*PNT.alpha₂-AP*, constructed as shown in figure 4, the *neomycin resistance* expression cassette replaces a 7 kb genomic fragment comprising exon 2 through part of exon 10 (including the stop codon) (figure 5). This represents a deletion of the entire sequence encoding the mature protein (36).

The NotI-linearized targeting vector was electroporated in R₁ ES cells and Southern blot analysis of genomic DNA identified 3 correctly targeted clones. Correctly targeted clones displayed the expected fragments after Southern blot analysis for the 5' end with probe A or probe B (data not shown) of EcoRV-restricted genomic DNA. Likewise, Southern blot analysis for the 3' end using probe C yielded an 8 kb *Kpn*I wild-type and a 5 kb *Kpn*I mutant fragment. Southern blot analysis of ScaI-restricted genomic DNA with the probe D generated a single 6.0 kb mutant fragment, indicating single integration of the targeting construct at the *AP* locus.

5.3. Germline transmission of the inactivated *alpha₂-antiplasmin* gene

Morula aggregation of recombinant RW4 cell clones harboring a disrupted *AP* gene, yielded germline-competent chimeras (male), as indicated by the presence of agouti pups among their offspring after mating with C57BL6/J females. Heterozygous AP-deficient (AP⁺ᐟ⁻) mice among the agouti offspring were identified by Southern blot analysis of tail tip DNA and were intercrossed, yielding AP⁺ᐟ⁺, AP⁺ᐟ⁻ and AP⁻ᐟ⁻ F₂ littermates, in a genetic background of 50% 129/SvJ and 50% C57BL6/J.

Deficiency in AP in the AP⁻ᐟ⁻ progeny was confirmed at the mRNA level by the absence of signal in RT.PCR analyses of kidney and liver polyA RNA using primers annealing in the coding part of exon 10 (27,36).

6. PHENOTYPIC ANALYSIS

All animals were kept in microisolation cages on a 12 h day-night cycle and fed regular chow. All experiments were approved by the local ethical committee and were performed in accordance with the guiding principles of the American Physiological Society and the International Society on Thrombosis and Hemostasis.
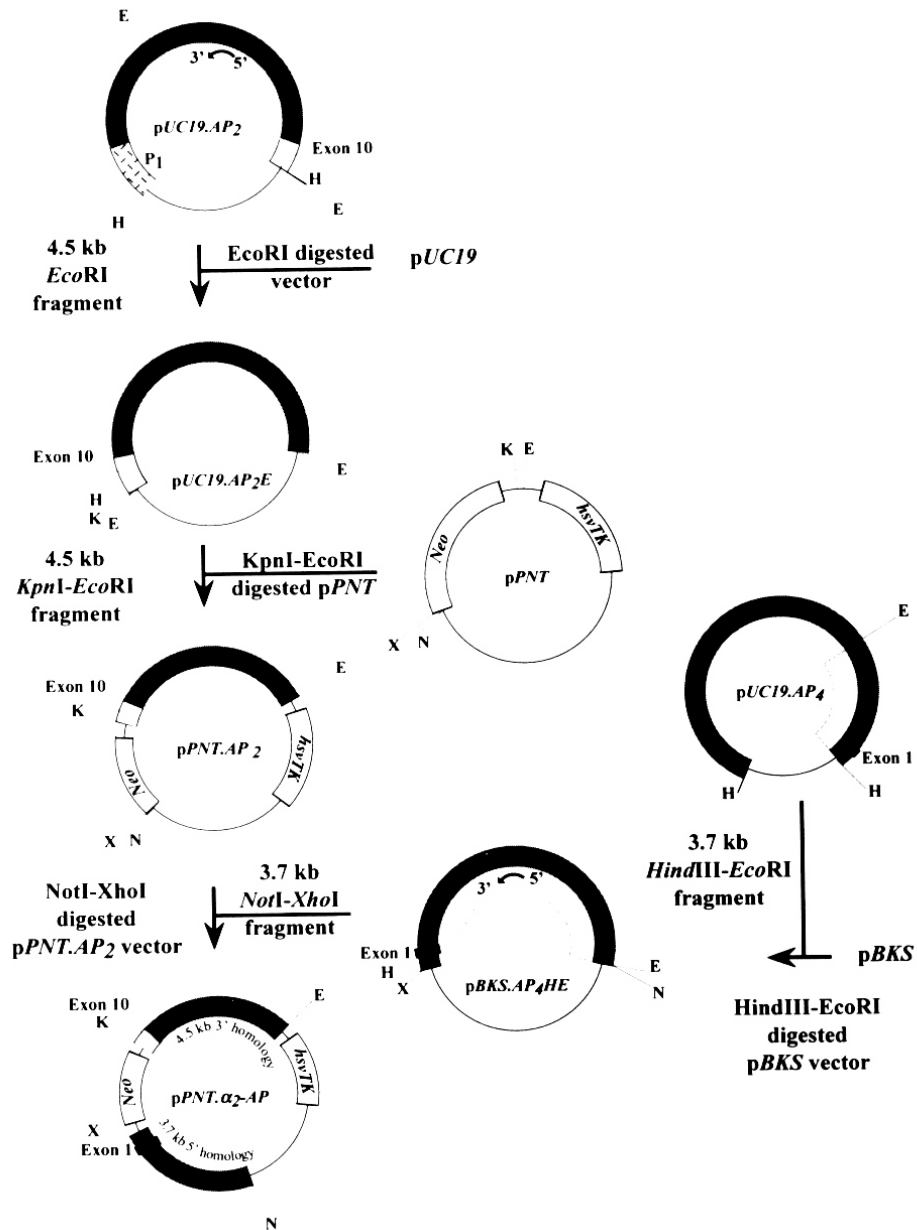
Alpha$_2$-antiplasmin

Figure 4. Outline of the construction of the *AP* targeting vector p*PNT alpha$_2$-AP*. Restriction fragments used in the constructions are indicated by a dashed line on the original plasmid. Bacterial sequences in the plasmids are indicated by a thin line. Black boxes represent *AP* coding sequences; open boxes, untranslated exon sequences; shaded boxes represent intron sequences; the cross-hatched box in p*UC19.AP$_2$* represents sequences originating from the P$_1$ phage (reproduced from ref. 36, with permission).E: EcoRI; H: HindIII; K: KpnI; N:NotI; X: XhoI.

6.1. Viability, fertility and growth

Among 161 F$_2$ littermates from heterozygous crosses that were genotyped at 4 to 5 weeks of age, 23% were *AP$^{+/+}$*, 53% were *AP$^{+/-}$* and 24% were *AP$^{-/-}$*. This distribution is similar for males and females, and is not significantly different from the expected Mendelian 1:2:1 ratio, thus indicating equal viability (27).

AP deficiency did not affect the growth rate of the mice, as evidenced by weighing the mice at weekly intervals. Body weights at 5 weeks of age were (mean ± SEM; n= 4), 17 ± 2 g and 15 ± 1 g for AP$^{+/+}$ and AP$^{-/-}$ mice respectively, with corresponding values of 22 ± 2 g and 23 ± 1 g at 10 weeks. Mean body weights of AP$^{+/-}$ mice (mean ± SEM; n= 13) were 16 ± 1 g and 22 ± 4 g at 5 and 10 weeks of age, respectively. No macroscopic abnormalities were observed. AP$^{-/-}$ mice (F$_2$ and F$_3$ generations) produced similar sizes of litters as AP$^{+/+}$ mice (8 ± 1 or 7 ± 1 mice per litter); the time between litters was however somewhat longer for the AP$^{-/-}$ breeding pairs (30 ± 3 versus 29 ± 3 days) (p = 0.011).
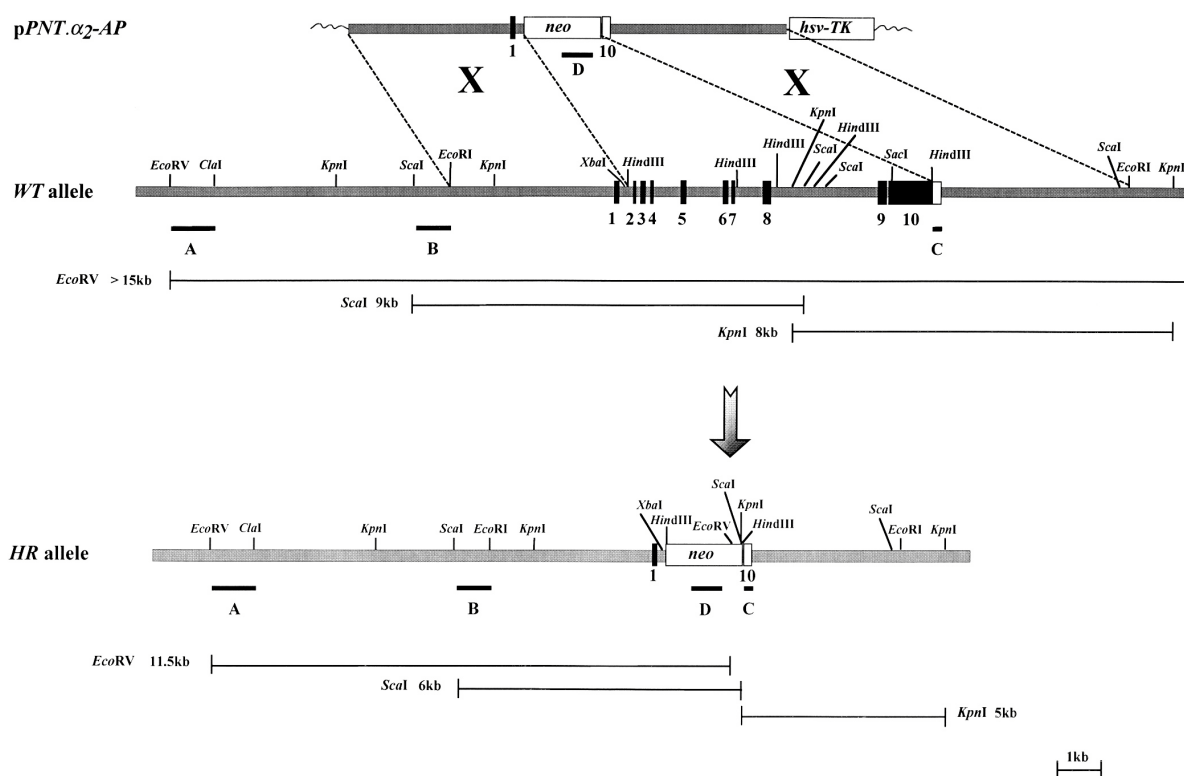
244

Figure 5. Outline of the strategy to inactivate the murine *AP* gene by homologous recombination in embryonic stem cells. The targeting vector p*PNT*. alpha$_2$*AP*, the wild-type *AP* allele and the homologously recombined allele are schematically represented. The targeting vector contains the *neomycin resistance* gene (*neo*) and the *Herpes simplex virus thymidine kinase* gene (*hsv-TK*) to allow for double selection of homologous recombination events. Expression of *neo* and *hsv-TK* was under the control of the *phosphoglycerokinase* promoter. Transcription of both selectable markers was in the same direction as the endogenous *AP* gene. Black boxes in the genomic structures represent coding exon sequences, open boxes represent non-coding exon sequences. Upon homologous recombination, the *neo* gene replaces a 7 kb genomic fragment comprising exon 2 through part of exon 10 (including the stop codon). The expected restriction fragments of the wild-type and the mutant allele are indicated with their relative size by underlining. Black boxes under the genes represent the probes used for Southern blot analysis. Probe A is a 1 kb *Eco*RV-*Cla*I genomic fragment prepared from p*UC19.AP$_4$* and located approximately 5 kb upstream of the 5' flanking region. Probe B is a 0.9 kb *Sca*I-*Eco*RI genomic fragment located immediately upstream of the 5' flanking region. Probe C is a 0.2 kb amplification product obtained from genomic DNA by PCR, corresponding to the exon 10 sequences comprised in the 3' flanking region. Probe D is a 0.6 kb *Pst*I fragment from the *neo* gene (reproduced from ref. 36, with permission).

AP antigen levels in plasma were gene-dose-dependent. The functional assay revealed an unexpectedly high level of antiplasmin activity in AP$^{-/-}$ plasma as compared to AP$^{+/-}$ and AP$^{+/+}$ plasma: $22 \pm 3\%$ (mean $\pm$ SEM; n= 14) versus $47 \pm 5\%$ (n= 10) and $94 \pm 5\%$ (n= 13), respectively. The levels in male or female AP$^{-/-}$ mice were not significantly different: $18 \pm 4.4\%$ versus $26 \pm 4.0\%$ (n= 7; p= 0.16). This rapid reacting plasmin inhibitory activity cannot be due to murine AP activity, because no complexes corresponding to plasmin-AP could be detected upon addition of murine or human plasmin to AP$^{-/-}$ plasma (27).

Plasma levels of alpha$_2$-macroglobulin antigen were higher in AP$^{-/-}$ mice than in AP$^{+/+}$ mice, for females ($128 \pm 7\%$, n= 10, versus $101 \pm 5\%$, n= 7, p= 0.02), and for males ($134 \pm 13\%$, n= 10, versus $100 \pm 9\%$, n= 6; p= 0.12). All other measured haemostasis parameters (plasminogen, fibrinogen, PAI-1, haemoglobin, haematocrit) and cell counts (red and white blood cells and platelets) were comparable for AP$^{+/+}$, AP$^{+/-}$ and AP$^{-/-}$ mice.

Bleeding times after amputation of a toe were very variable (range $0.5 - 7$ min) but were on average (mean $\pm$ SEM) not significantly different between AP$^{+/+}$ (210 ± 64 s; n= 5), AP$^{+/-}$ (180 ± 37 s; n= 12) and AP$^{-/-}$ (210 ± 72 s; n= 5) mice. Also after tail amputation bleeding stopped spontaneously in all 3 genotypes. No significant rebleeding was observed (27).

6.2. Endogenous thrombolytic potential

Spontaneous lysis within 2 to 4 h of a ^{125}I-fibrin labeled pulmonary plasma clot was always higher in AP$^{-/-}$ than in AP$^{+/+}$ mice. In AP$^{+/+}$ mice, lysis of a clot produced from AP$^{+/+}$ or from AP$^{-/-}$ plasma was comparable, indicating that the AP content of the clot does not significantly inhibits lysis in plasma with normal inhibitor concentration. Also in AP$^{-/-}$ mice, lysis of both clot types was not significantly different (27).

6.3. Renal thrombosis

Histopathological examination and immunostaining of kidney sections after endotoxin injection in AP$^{+/+}$ mice revealed the occasional presence of fibrin deposits in the glomeruli of the outer cortex and, more frequently, in the capillaries of the medulla. In AP$^{+/+}$ mice without endotoxin injection and in AP$^{-/-}$ mice after endotoxin injection, significantly less fibrin deposits were detected in the glomeruli and in the medulla. Semi-quantitative analysis of fibrin deposition in the glomeruli indicated that, 8 h after endotoxin injection, all 15 sections of AP$^{-/-}$ mice (4 animals) were free of fibrin, whereas only 9 out of 16 sections of AP$^{+/+}$ mice were devoid of fibrin. In the capillaires of the medulla, fibrin deposits were detected in 4 of 15 sections of AP$^{-/-}$ mice, whereas 14 of 16 sections of AP$^{+/+}$ mice revealed fibrin deposition. This represents a significant reduction of fibrin deposits in AP$^{-/-}$ mice as compared to AP$^{+/+}$ mice (27).

6.4. Arterial thrombosis

Thrombosis was photochemically induced in the murine carotid artery and platelet-rich thrombus formation was continuously monitored via transillumination and quantitated by image analysis. The sizes of thrombi developing in AP$^{+/+}$, in AP$^{+/-}$ and in AP$^{-/-}$ mice were 102 ± 35, 65 ± 8.1 and 13 ± 6.1 million A.U. respectively (n= 6 each). These findings confirmed that during acute thrombus development, plasmin is locally formed and inhibited by AP (38).

6.5. Neointima formation after vascular injury

The hypothesis that AP plays a role in neointima formation was tested with the use of a vascular injury model in AP$^{+/+}$ and AP$^{-/-}$ mice. The neointimal and medial areas at 1 to 3 weeks after electric injury of the femoral artery were similar in AP$^{+/+}$ and AP$^{-/-}$ mice, resulting in comparable intima/media ratios (e.g. 0.43 ± 0.12 and 0.42 ± 0.11 at 2 weeks after injury). Nuclear cell counts in cross-sectional areas of the intima of the injured region were also comparable in AP$^{+/+}$ and AP$^{-/-}$ arteries (78 ± 19 and 69 ± 8). Fibrin deposition was not significantly different in arteries of both genotypes at 1 day after injury, and no mural thrombosis was detected at 1 week after injury. Fibrinolytic activity in femoral arterial sections, as monitored by fibrin zymography, was higher in AP$^{-/-}$ arteries at 1 week after injury (p < 0.001), but was comparable in both genotypes at 2 and 3 weeks after injury. Staining for elastin did not reveal significant degradation of the internal elastica lamina in either genotype. Immunocytochemical analysis revealed a comparable distribution pattern of alpha-actin-positive smooth muscle cells (SMC) in both genotypes (39).

In another study, the left common carotid artery of C57BL/6J mice was ligated proximal to the bifurcation. On day 3 after ligation, in addition to infiltrated granulocytes, platelet micro-thrombi and platelet-covered leukocytes as well as tissue factor positive fibrin deposits were found lining the endothelium; leukocyte tissue factor in the vessel wall lumen progressively increased over 2 weeks. Neointima formation in control mice, evaluated by computerized morphometry of carotid artery cross-sections, equaled $28 \pm 3.7\%$ (n= 11) and $42 \pm 5.1\%$ (n= 8) one and two weeks after ligation. In AP$^{-/-}$ mice, luminal stenosis was lower at one week ($14 \pm 2.6\%$, n= 7, p < 0.01), but not at two weeks (40).

These findings indicate that the endogenous fibrinolytic system of the AP$^{+/+}$ mice is capable of preventing fibrin deposition after vascular injury, and suggest that AP does not play a major role in SMC migration and neointima formation in vivo.

6.6. Stroke

Focal cerebral ischemia was produced by ligation of the left middle cerebral artery (MCA) in mice and cerebral infarct size was measured after 24 hours by planimetry of 2,3,5-triphenyltetrazoliumchloride stained brain slices. AP$^{-/-}$ mice had smaller infarcts (2.2 ± 1.1 mm^3, p < 0.0001 vs AP$^{+/+}$), which increased to 13 ± 2.5 mm^3 following intravenous injection of 1.0 mg purified human AP (p < 0.005 vs AP$^{-/-}$). Injection in AP$^{-/-}$ mice of 0.7 to 2.1 mg Fab fragments of affino-specific polyclonal rabbit IgG against human AP, 15 min after injection of 200 µg human AP, reduced infarct size from 9.0 ± 1.9 mm^3 to 4.5 ± 1.9 mm^3 (p= 0.09). The observation that inhibition of AP reduces infarct size, suggests a potential avenue to counteract focal ischemic cerebral infarction (41).

7. REFERENCES

1. Lijnen H R, & D. Collen: Mechanisms of physiological fibrinolysis. *Baillière's Clinical Haematology* 8, 277-290 (1995)

2. Holmes W E, L. Nelles, H. R. Lijnen & D. Collen: Primary structure of human alpha2-antiplasmin, a serine protease inhibitor (serpin). *J Biol Chem* 262, 1659-1664 (1987)

3. Lijnen H R, W. E. Holmes, B. Van Hoef, B. Wiman, H. Rodriguez & D. Collen: Amino-acid sequence of human alpha2-antiplasmin. *Eur J Biochem* 166, 565-574 (1987)

4. Christensen S, L. Berglund & L. Sottrup-Jensen: Primary structure of bovine alpha-2-antiplasmin. *FEBS Lett* 343, 223-228 (1994)

5. Bangert K, A. H. Johnsen, U. Christensen & S. Thorsen: Different N-terminal forms of alpha2-plasmin inhibitor in human plasma. *Biochem J* 291, 623-625 (1993)

6. Kimura S & N. Aoki: Cross-linking site in fibrinogen for alpha2-plasmin inhibitor. *J Biol Chem* 261, 15591-15595 (1986)

7. Sumi Y, Y. Ichikawa, Y. Nakamura, O. Miura & N. Aoki: Expression and characterization of pro alpha2-plasmin inhibitor. *J Biochem* (Tokyo) 106, 703-707 (1989)

8. Wiman B & D. Collen: Purification and characterization of human antiplasmin, the fast-acting plasmin inhibitor in plasma. *Eur J Biochem* 8, 19-26 (1977)

9. Collen D & B. Wiman: Turnover of antiplasmin, the fast-acting plasmin inhibitor of plasma. *Blood* 53, 313-324 (1979)

10. Christensen U & I. Clemmensen: Purification and reaction mechanisms of the primary inhibitor of plasmin from human plasma. *Biochem J* 175, 635-641 (1978)

11. Sugiyama N, T. Sasaki, M. Iwamoto & Y. Abiko: Binding site of alpha2-plasmin inhibitor to plasminogen. *Biochim Biophys Acta* 952, 1-7 (1988)

12. Wiman B, T. Nilsson & B. Cedergren: Studies on a form of alpha2-antiplasmin in plasma which does not interact with the lysine-binding sites in plasminogen. *Thromb Res* 28, 193-200 (1982)

13. Christensen U, & I. Clemmensen: Kinetic properties of the primary inhibitor of plasmin from human plasma. *Biochem J* 163, 389-391 (1977)

14. Wiman B & D. Collen: On the kinetics of the reaction between human antiplasmin and plasmin. *Eur J Biochem* 84, 573-578 (1978)

15. Wiman B, L. Boman & D. Collen: On the kinetics of the reaction between human antiplasmin and a low-molecular-weight form of plasmin. *Eur J Biochem* 87, 143-146 (1978)

16. Wiman B, H. R. Lijnen & D. Collen: On the specific interaction between the lysine-binding sites in plasmin and complementary sites in alpha2-antiplasmin and in fibrinogen. *Biochim Biophys Acta* 579, 142-154 (1979)

17. Wiman B & D. Collen: On the mechanism of the reaction between human alpha2-antiplasmin and plasmin. *J Biol Chem* 254, 9291-9297 (1979)

18. Holmes W E, H. R. Lijnen & D. Collen: Characterization of recombinant human alpha2-antiplasmin and of mutants obtained by site-directed mutagenesis of the reactive site. *Biochemistry* 26, 5133-5140 (1987)

19. Lijnen H R, B. Van Hoef, V. Beelen & D. Collen: Characterization of the murine plasma fibrinolytic system. *Eur J Biochem* 224, 863-871 (1994)

20. Wiman B & D. Collen: Molecular mechanism of physiological fibrinolysis. *Nature* 272, 549-550 (1978)

21. Kato A, S. Hirosawa, S. Toyota, Y. Nakamura, H. Nishi, A. Kimura, T. Sasazuki & N. Aoki: Localization of the human alpha2-plasmin inhibitor gene (PLI) to 17 p 13. Cytogenet Cell Genet 62, 190-191 (1993)

22. Hirosawa S, Y. Nakamura, O. Miura, Y. Sumi & N. Aoki: Organization of the human   alpha2-plasmin inhibitor gene. *Proc Natl Acad Sci USA* 85, 6836-6840 (1988)

23. Koie K, K. Ogata, T. Kamiya, J. Takamatsu & M. Kohakura: Alpha2-plasmin-inhibitor deficiency (Miyasato disease). *Lancet* 2, 1334-1336 (1978)

24. Lijnen H R & D. Collen: Congenital and acquired deficiencies of components of the fibrinolytic system and their relation to bleeding or thrombosis. *Fibrinolysis* 3, 67-77 (1989)

25. Miura O, Y. Sugahara & N. Aoki: Hereditary alpha2-plasmin inhibitor deficiency caused by a transport-deficient mutation (alpha2-PI-Okinawa). Deletion of Glul37 by a trinucleotide deletion blocks intracellular transport. *J Biol Chem* 264, 18213-18219 (1989)

26. Miura O, S. Hirosawa, A. Kato & N. Aoki: Molecular basis for congenital deficiency of alpha2--plasmin inhibitor. A frameshift mutation leading to elongation of the deduced amino acid sequence. *J Clin Invest* 83, 1598-1604 (1989)

27. Lijnen H R, K. Okada, O. Matsuo, D. Collen & M. Dewerchin: Alpha2--antiplasmin gene deficiency is associated with enhanced fibrinolytic potential without overt bleeding. Blood 93, 2274-2281 (1999)

28. Teger-Nilsson A C, E. Gyzander, H. Myrwold, H. Noppa, R. Olsson & L. Wallmo: Determination of fast-acting plasmin inhibitor (alpha2-antiplasmin) in plasma from patients with tendency to thrombosis and increased fibrinolysis. *Haemostasis* 7, 155-157 (1978)

29. Aoki N & T. Yamanaka: The alpha2-plasmin inhibitor levels in liver diseases. *Clin Chim Acta* 84, 99-105 (1978)

30. Högstorp H, H. Jacobsson & T. Saldeen: Effect of hepatectomy on the posttraumatic fibrinolysis inhibition and the primary fibrinolysis inhibitor in the rat. Thromb Res 18, 361-368 (1980)

31. Collen D & H. R. Lijnen: The fibrinolytic system in man. *CRC Crit Rev Oncol Hematol* 4, 249-301 (1986)

32. Collen D, H. Bounameaux, F. De Cock, H. R. Lijnen & M. Verstraete: Analysis of coagulation and fibrinolysis during intravenous infusion of recombinant human tissue-type plasminogen activator in patients with acute myocardial infarction. *Circulation* 73, 511-517 (1986)

33. Kluft C, H. K. Nieuwenhuis, D. C. Rijken, E. Groeneveld, G. Wijngaards, W. van Berkel, G. Dooijewaard & J.J. Sixma: Alpha 2-antiplasmin Enschede : dysfunctional alpha 2-antiplasmin molecule associated with an autosomal recessive hemorrhagic disorder. *J Clin Invest* 80, 1391-1400 (1987)

34. Holmes W E, H. R. Lijnen, L. Nelles, C. Kluft, H. K. Nieuwenhuis, D. C. Rijken & D. Collen: Alpha--antiplasmin Enschede: alanine insertion and abolition of plasmin inhibitory activity. *Science* 238, 209-211 (1987)

35. Menoud P A, N. Sappino, M. Boudal-Khoshbeen, J. D. Vassalli & A. P. Sappino: The kidney is a major site of alpha2-antiplasmin production. *J Clin Invest* 97, 2478-2484 (1996)

36. Okada K, H. R. Lijnen, M. Dewerchin, A. Belayew, O. Matsuo, D. Collen & R. Bernaerts: Characterization and targeting of the murine alpha2-antiplasmin gene. *Thromb Haemost* 78, 1104-1110 (1997)

37. Klug J & M. Beato: Binding of YY1 to a site overlapping a weak TATA box is essential for transcription from the uteroglobin promoter in endometrial cells. *Mol Cell Biol* 16, 6398-6407 (1996)

38. Kawasaki T, M. Dewerchin, H. R. Lijnen, J. Vermylen & M. F. Hoylaerts: Vascular release of PAI-1 impairs fibrinolysis during acute arterial thrombosis in mice. *Blood* 96, 153-160 (2000)

39. Lijnen H R, B. Van Hoef, M. Dewerchin & D. Collen: Alpha2-antiplasmin gene deficiency in mice does not affect neointima formation after vascular injury. *Arterioscler Thromb Vasc Biol*, 20, 1488-1492 (2000)

40. Kawasaki T, M. Dewerchin, H. R. Lijnen, I. Vreys, J. Vermylen & M. F. Hoylaerts: Mouse carotid artery ligation induces platelet-leukocyte dependent luminal fibrin, required for neointima development.*Circ Res*, in press.

41. Nagai N, M. De Mol, H. R. Lijnen, P. Carmeliet & D. Collen: Role of plasminogen system components in focal cerebral ischemic infarction. A gene targeting and gene transfer study in mice. *Circulation* 99, 2440-2444 (1999)

Send correspondence to: H.R. Lijnen, Center for Molecular and Vascular Biology, University of Leuven, Campus Gasthuisberg, O & N,Herestraat 49, B-3000 Leuven, Belgium, Tel: 32-16-345771, Fax: 32-16-345990, E-mail: roger.lijnen@med.kuleuven.ac.be